RSC Advances

ROYAL SOCIETY OF CHEMISTRY

www.rsc.org/advances

Table of Contents

Four Benzo[1,2-b:4,5-b′]dithiophene (BDT) centred small molecules with different acceptor and end-capping groups were synthesized as the donor materials for organic solar cells

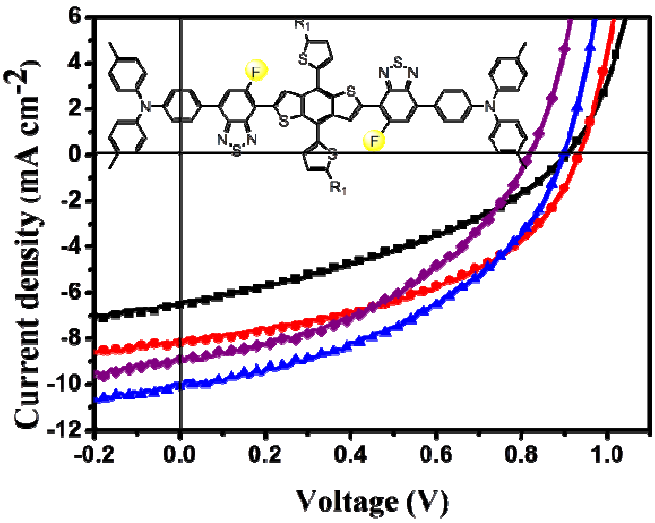

Cite this: DOI: 10.1039/c0xx00000x

www.rsc.org/xxxxxx

ARTICLE TYPE

Synthesis, characterization and photovoltaic properties of benzo[1,2-*b*:4,5-*b′*]dithiophene-bridged molecules†

Xinli Liu,[a,b] Shusheng Li,[c] Jinhua Li,[d] Jian Wang,[e] Zhan'ao Tan,*[c] Feng Yan,[d] Hua Li,[b,f] Yih Hsing Lo,*[g] Chung-Hin Chui,[h] and Wai-Yeung Wong*[b]

Received (in XXX, XXX) Xth XXXXXXXXX 20XX, Accepted Xth XXXXXXXXX 20XX
DOI: 10.1039/b000000x

Four new acceptor-donor-acceptor based organic small molecules with benzo[1,2-*b*:4,5-*b′*]dithiophene (BDT) unit as the central donor group, benzothiadiazole (BT) or fluoro-substituted benzothiadiazole as the acceptor, and different end-capping groups (**BTBDT1**–**BTBDT4**) have been synthesized and tested for solution-processed bulk-heterojunction organic solar cells. The absorption spectra, electronic energy levels, hole mobilities and solar cell performance of these compounds were investigated. All compounds show broad absorption in the visible range. The PCE of the solar cell device based on **BTBDT3**/$PC_{71}BM$ (1:2, w/w) reached 3.91% with a J_{sc} of 10.08 mA cm^{-2}, a V_{oc} of 0.90 V and a FF of 0.43, under illumination of AM 1.5 G, 100 mW cm^{-2}.

Introduction

For the rational exploitation of solar energy, organic solar cells (OSCs), with a number of advantages such as low-cost, light weight, and large-area fabrication on flexible substrates, have been developing at a quick pace in the past few years.[1–9] Among various potential materials used in OSCs, an encouraging power conversion efficiency (PCE) of over 10% has been achieved by polymer materials in bulk heterojunction (BHJ) OSCs.[10] On the other hand, organic small molecules have attracted considerable recent attention because of their advantages such as well-defined molecular structure, synthetically high reproducibility and no batch to batch variations, etc. as compared to the organic polymeric materials.[11–13] A variety of organic small molecules containing oligothiophenes,[14] diketopyrrolopyrroles,[15] triphenylamine,[16] benzothiadiazole (BT),[17] thiazolothiazole,[18] dithieno[3,2-*b*:2′3′-*d*]silole[19] and organic dyes[20] have been broadly researched as photovoltaic materials for OSCs. Up till now, a PCE over 8% has been achieved by using organic small molecule p-DTS(FBTTh$_2$)$_2$ with acceptor-donor-acceptor (A-D-A) structural motif as n-type material for OSCs.[21] Noticeably, the PCEs of organic small molecules are still below their polymeric counterparts.[22] On the other hand, organic small molecules with D-A architecture have been continually studied due to the easy tailoring of their electronic structures, and many efforts have been applied to the design and synthesis of new donor and acceptor building blocks. Among them, benzo[1,2-*b*:4,5-*b′*]dithiophene (BDT) unit is a good electron-donating group and it has been emerging recently as an attractive donor building block in organic polymer materials for high performance OSCs because of its rigid coplanar fused ring structure, which easily gives rise to high π-electron delocalization and strong intermolecular π-π stacking.[14b, 23] Also, BDT-based polymers show a more harmonious relationship between band gap and HOMO energy level than other widely used π-conjugated blocks for building polymeric OSC materials. Moreover, upon introducing a thiophene unit onto the BDT side position (BDT-T) for enlarging the molecular π-overlap, the performance of related donor materials may be further enhanced.[24]

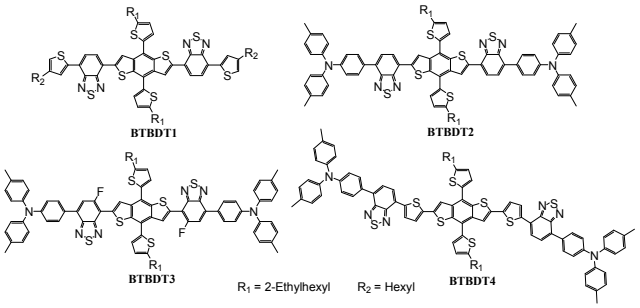

Fig. 1 Molecular structures of **BTBDT1**, **BTBDT2**, **BTBDT3** and **BTBDT4**.

Here, we report a series of A-D-A organic small molecules consisting of alkylthiophene substituted BDT (BDT-T) unit as a central donor (D), benzothiadiazole (BT) or monofluoro-substituted BT (F-BT) unit as an acceptor (A) and alkylthiophene unit or *N,N*-di-*p*-tolylbenzenamine unit as an end-capping group. Fig. 1 shows the chemical structures of these new molecules. Except for **BTBDT1** constructed with 3-hexylthiophene unit as

the end-capping groups, **BTBDT2**, **BTBDT3** and **BTBDT4** were built by the *N,N*-di-*p*-tolylbenzenamine terminal unit to study the effects of such end group on the OSC performance and hole mobility property. Also, **BTBDT3** was investigated by using fluorine-substituted BT unit to replace the original BT unit in **BTBDT2** (Fig. 1) to investigate the fluorination effects on both OSC and OFET performance, as it is known that fluorine atom normally plays a crucial role in OSC materials because of its unique features including the high stability against oxidation, elevated resistance to degradation, higher hydrophobicity and larger effect on inter- and intra-molecular interaction via C–F···H, F···S and C–F···π_F interactions.[25] All the materials synthesized showed strong absorption between 300 and 650 nm in solid films, corresponding to the optical band-gap energy between 1.65 and 1.72 eV, which is suitable for OSC application. As a result a PCE of 3.91% was achieved for solution-processed OSCs based on a blend of **BTBDT3**/phenyl C_{71}-butyric acid methyl ester ($PC_{71}BM$) without the need of any post-treatment such as addition of additives and thermal annealing. Thus, alkylthiophene-substituted BDT is a promising donor building block for efficient small-molecule OSCs.

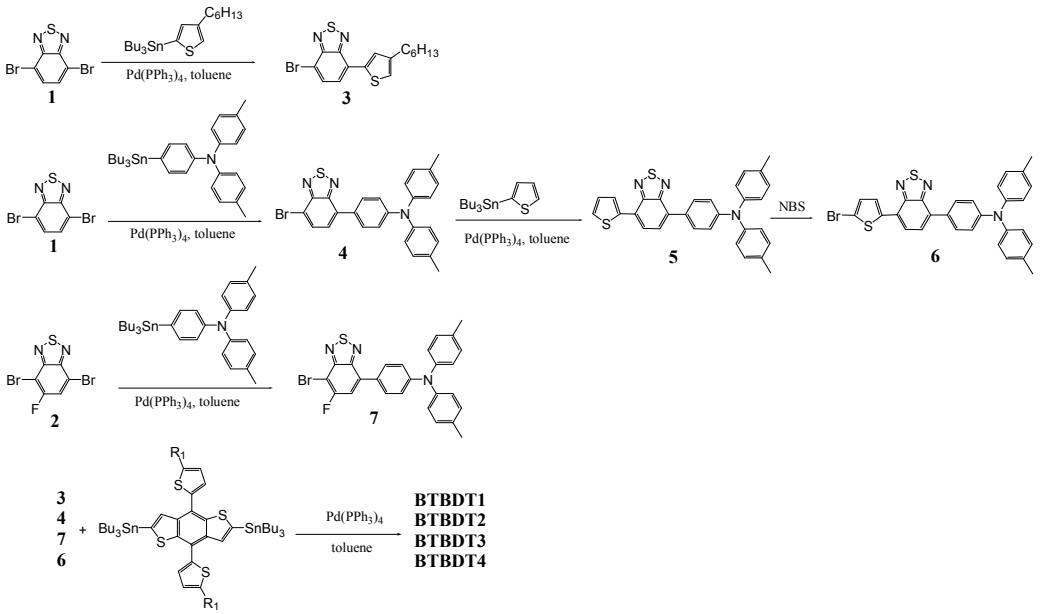

Scheme 1 Synthetic routes for **BTBDT1–BTBDT4**.

Experimental section

Materials and methods

All reactions were carried out under a nitrogen atmosphere. All reagents and chemicals were purchased from commercial sources and used without further purification. Toluene was dried over Na/benzophenone ketyl and freshly distilled prior to use.

Synthesis

4,7-Dibromo-5-fluorobenzo[*c*][1,2,5]thiadiazole (**2**), 4-bromo-7-(4-hexylthiophen-2-yl)benzo[*c*][1,2,5]thiadiazole (**3**), BDT-tributylstannane and *N*-(4-(tributylstannyl)phenyl)-4-methyl-*N*-*p*-tolylbenzenamine were synthesized following the literature methods.[21,26]

Synthesis of BTBDT1

To a 100 mL round-bottom flask was added $Pd(PPh_3)_4$ (25 mg, 0.02 mmol), **3** (0.41 g, 1.1 mmol) and BDT-based bis(tributylstannane) (0.57 g, 0.5 mmol) in toluene (30 mL). The mixture was heated to reflux for 48 h under a nitrogen atmosphere. After removal of the solvents, the crude product was purified by column chromatography on silica gel eluting with hexane/CH_2Cl_2 (4:1 to 2:1, v/v) solvent mixture to give a brown solid (0.2 g, 34%).

^{1}H NMR (400 MHz, $CDCl_3$): δ = 8.72 (s, 2H, Ar), 7.79 (s, 2H, Ar), 7.69 (d, 2H, *J* = 7.6 Hz, Ar), 7.65 (d, 2H, *J* = 7.6 Hz, Ar), 7.38 (d, 2H, *J* = 3.4 Hz, Ar), 6.93 (d, 2H, *J* = 3.4 Hz, Ar), 6.89 (s, 2H, Ar), 2.90 (d, 4H, *J* = 6.8 Hz, alkyl), 2.55 (t, 4H, *J* = 7.8 Hz, alkyl), 1.76–1.70 (m, 4H, alkyl), 1.58–1.54 (m, 8H, alkyl), 1.44–1.24 (m, 28H, alkyl), 0.97 (t, 6H, *J* = 7.2 Hz, alkyl), 0.89 (t, 6H, *J* = 7.0 Hz, alkyl), 0.83 (t, 6H, *J* = 6.8 Hz, alkyl); ^{13}C NMR (100 MHz, $CDCl_3$): 151.1, 144.1, 142.7, 137.9, 137.5, 136.7, 136.3, 136.2, 127.2, 127.1, 125.3, 124.8, 124.2, 123.6, 123.5, 123.0, 122.2, 120.0 (Ar), 40.5, 33.3, 31.6, 30.7, 29.4, 29.0, 28.2, 28.0, 24.7, 22.2, 21.6, 13.3, 13.1, 10.1 (alkyl) ppm. MALDI-TOF $[M+1]^+$: found: 1179.4, calcd: 1179.37. Anal. Calcd for $C_{66}H_{74}N_4S_8$: C, 67.21; H, 6.33; N, 4.75. Found: C, 67.34; H, 6.45; N, 4.98%.

Synthesis of 4

To a 100 mL round-bottom flask was added $Pd(PPh_3)_4$ (60 mg, 0.05 mmol) *N*-(4-(tributylstannyl)phenyl)-4-methyl-*N*-*p*-tolylbenzenamine (1.7 g, 3.0 mmol) and 4,7-dibromobenzothiadiazole (0.88 g, 3.0 mmol) in toluene (50 mL). The mixture was heated to reflux for 24 h under a nitrogen atmosphere. After removal of the solvents, the crude product was

purified by column chromatography on silica gel eluting with hexane/CH_2Cl_2 (5:1, v/v) solvent mixture and the desired product was isolated as a yellow solid (1.2 g, 82%).

^{1}H NMR (400 MHz, $CDCl_3$): δ = 7.28 (d, 1H, *J* = 3.8 Hz, Ar), 7.70 (d, 2H, *J* = 8.6 Hz, Ar), 7.45 (d, 1H, *J* = 3.4 Hz, Ar), 7.06–6.99 (m, 10H, Ar), 2.26 (s, 6H, Me); ^{13}C NMR (100 MHz, $CDCl_3$): 153.1, 148.4, 147.5, 147.3, 133.5, 132.4, 129.9, 129.8, 129.4, 129.3, 127.3, 125.1, 124.9, 123.3, 122.9, 122.6, 112.2 (Ar), 24.1 (Me) ppm. MALDI-TOF $[M+1]^+$: found: 486.1, calcd: 486.06.

Synthesis of BTBDT2

To a 100 mL round-bottom flask was added $Pd(PPh_3)_4$ (10 mg, 8 μmol), **4** (0.15 g, 0.31 mmol) and BDT-based bis(tributylstannane) (0.17 g, 0.15 mmol) in toluene (30 mL). The mixture was heated to reflux for 48 h under a nitrogen atmosphere. After removal of the solvents, the crude product was purified by column chromatography on silica gel eluting with hexane/$CHCl_3$ (4:1 to 2:1, v/v) solvent mixture to afford a brown solid (75 mg, 36%).

^{1}H NMR (400 MHz, $CDCl_3$): δ = 8.83 (s, 2H, Ar), 7.88 (d, 2H, *J* = 3.8 Hz, Ar), 7.77 (d, 4H, *J* = 8.6 Hz, Ar), 7.61 (d, 2H, *J* = 3.4 Hz, Ar), 7.06–6.92 (m, 20H, Ar), 2.88, (d, 4H, *J* = 6.8 Hz, alkyl), 2.27 (s, 12H, Me), 1.70 (br, 2H, alkyl), 1.57–1.36 (m, 18H, alkyl), 0.94 (t, 6H, *J* = 7.2 Hz, alkyl), 0.86 (t, 6H, *J* = 6.8 Hz, alkyl); ^{13}C NMR (100 MHz, $CDCl_3$): 152.7, 151.7, 147.3, 144.5, 143.8, 138.8, 137.3, 136.7, 136.3, 131.9, 131.8, 128.8, 128.5, 128.3, 126.9, 126.2, 125.5, 124.4, 124.1, 123.9, 123.3, 122.7, 120.3 (Ar), 40.5, 33.3, 31.6, 27.9, 24.7 (Me), 22.1, 19.8, 13.2, 10.1 (alkyl) ppm. MALDI-TOF $[M+1]^+$: found: 1389.5, calcd: 1389.48. Anal. Calcd for $C_{86}H_{80}N_6S_6$: C, 74.33; H, 5.81; N, 6.05. Found: C, 74.40; H, 5.99; N, 5.95%.

Synthesis of 7

To a 100 mL round-bottom flask was added $Pd(PPh_3)_4$ (100 mg, 0.08 mmol) *N*-(4-(tributylstannyl)phenyl)-4-methyl-*N*-*p*-tolylbenzenamine (2.2 g, 3.9 mmol) and 4,7-dibromo-5-fluorobenzothiadiazole (1.2 g, 3.9 mmol) in toluene (50 mL). The mixture was heated to reflux for 24 h under a nitrogen atmosphere. After removal of the solvents, the crude product was purified by column chromatography on silica gel eluting with hexane/CH_2Cl_2 (5:1, v/v) solvent mixture and a yellow solid was obtained (1.1 g, 56%).

^{1}H NMR (400 MHz, $CDCl_3$): δ = 7.78 (d, 2H, *J* = 8.9 Hz, Ar), 7.50 (d, 2H, *J* = 10.1 Hz, Ar), 7.11–7.06 (m, 10H, Ar), 2.33 (s, 6H, Me); ^{13}C NMR (100 MHz, $CDCl_3$): 162.2, 159.6, 154.5, 154.4, 150.3, 149.4, 144.6, 134.3, 134.2, 133.5, 130.1, 127.3, 127.2, 125.5, 120.9, 95.7, 95.5 (Ar), 19.8 (Me) ppm. MALDI-TOF $[M+1]^+$: found: 504.0, calcd: 504.02.

Synthesis of BTBDT3

To a 100 mL round-bottom flask was added $Pd(PPh_3)_4$ (10 mg, 8 μmol), **7** (0.25 g, 0.49 mmol) and BDT-based bis(tributylstannane) (0.26 g, 0.23 mmol) in toluene (30 mL). The mixture was heated to reflux for 48 h under a nitrogen atmosphere. After removal of the solvents, the crude product was purified by column chromatography on silica gel eluting with hexane/$CHCl_3$ (4:1 to 2:1, v/v) solvent mixture, yielding a brown solid (75 mg, 36%).

^{1}H NMR (400 MHz, $CDCl_3$): δ = 8.67 (s, 2H, Ar), 7.60 (d, 2H, *J* = 8.4 Hz, Ar), 7.39 (br, 4H, Ar), 6.96–6.89 (m, 22H, Ar), 2.88, (d, 4H, *J* = 6.8 Hz, alkyl), 2.24 (s, 12H, Me), 1.69 (br, 2H, alkyl), 1.49–1.32 (m, 18H, alkyl), 1.17 (s, 4H, alkyl), 0.99–0.87 (m, 12H, alkyl); ^{13}C NMR (100 MHz, $CDCl_3$): 160.3, 157.7, 152.8, 152.7, 149.9, 147.9, 144.6, 143.5, 138.3, 138.2, 136.2, 135.6, 132.7, 132.6, 132.3, 132.1, 131.9, 128.9, 128.6, 127.1, 126.7, 125.4, 125.3, 124.5, 124.3, 122.6, 119.9, 116.9, 116.7, 109.5, 109.3 (Ar), 40.5, 33.3, 31.6, 28.7, 28.0, 24.7 (Me), 22.1, 19.8, 13.2, 10.0 (alkyl) ppm. MALDI-TOF $[M+1]^+$: found: 1425.5, calcd: 1425.46. Anal. Calcd for $C_{86}H_{78}N_6F_2S_6$: C, 72.45; H, 5.52; N, 5.90. Found: C, 72.58; H, 5.69; N, 6.03%

Synthesis of 6

To **5** (0.1 g, 0.2 mmol) in 50 mL of $CHCl_3$/AcOH mixture solution was added NBS (36 mg, 0.2 mmol) at 0 °C. The mixture was stirred overnight and washed with water. After drying over Na_2SO_4, the residue was purified by silica gel chromatography using CH_2Cl_2:hexane (1:2, v/v) as eluent to give a red solid (90 mg, 79%).

^{1}H NMR (400 MHz, $CDCl_3$): δ = 7.84 (m, 3H, Ar), 7.80 (d, 1H, *J* = 3.4 Hz, Ar), 7.68 (d, 1H, *J* = 7.4 Hz, Ar), 7.15 (br, 3H, Ar), 7.12–7.09 (m, 8H, Ar), 2.33 (s, 6H, Me); ^{13}C NMR (100 MHz, $CDCl_3$): 153.8, 152.5, 148.6, 144.8, 140.9, 133.2, 132.9, 130.6, 130.0, 129.8, 129.4, 126.8, 125.5, 125.2, 124.6, 123.5, 121.4, 119.5, 114.1 (Ar), 20.8 (Me) ppm. MALDI-TOF $[M+1]^+$: found: 568.0, calcd: 568.04.

Synthesis of BTBDT4

To a 100 mL round-bottom flask was added $Pd(PPh_3)_4$ (15 mg, 13 μmol), **6** (0.25 g, 0.44 mmol) and BDT-based bis(tributylstannane) (0.24 g, 0.21 mmol) in toluene (30 mL). The mixture was heated to reflux for 48 h under nitrogen. After evaporation of the solvents, the crude product was purified by column chromatography on silica gel eluting with hexane/$CHCl_3$ (4:1 to 2:1, v/v) solvent mixture to furnish a brown solid (65 mg, 29%).

^{1}H NMR (400 MHz, $CDCl_3$): δ = 8.05 (d, 2H, *J* = 4.0 Hz, Ar), 7.91 (d, 2H, *J* = 7.4 Hz, Ar), 7.85 (d, 4H, *J* = 8.6 Hz, Ar), 7.77 (s, 2H, Ar), 7.69 (d, 2H, *J* = 7.6 Hz, Ar), 7.15–7.09 (m, 20H, Ar), 6.97 (d, 2H, *J* = 3.5 Hz, Ar), 2.94 (d, 4H, *J* = 6.8 Hz, alkyl), 2.33 (s, 12H, Me), 1.70 (br, 2H, alkyl), 1.57–1.36 (m, 16H, alkyl), 1.01–0.86 (m, 12H, alkyl); ^{13}C NMR (100 MHz, $CDCl_3$): 153.9, 152.7, 148.5, 146.0, 144.9, 138.4, 137.8, 137.4, 133.1, 129.9, 129.7, 129.5, 127.9, 126.9, 126.0, 125.5, 125.2, 124.9, 121.5, 119.3 (Ar), 41.5, 34.4, 32.6, 31.6, 29.0, 25.9, 23.1, 22.7 (Me), 20.9, 14.3, 14.2, 11.1(alkyl) ppm. MALDI-TOF $[M+1]^+$: found: 1553.5, calcd: 1553.46. Anal. Calcd for $C_{86}H_{78}N_6F_2S_6$: C, 72.66 H, 5.45; N, 5.41. Found: C, 72.50; H, 5.62; N, 5.60%.

Characterization

The high resolution matrix-assisted laser desorption/ionization time-of-flight (MALDI-TOF) spectra were obtained by an Autoflex Bruker MALDI-TOF mass spectrometer. NMR spectra were measured in deuterated solvents as the lock and reference on a Bruker AV 400 MHz FT-NMR spectrometer, with ^{1}H and ^{13}C NMR chemical shifts quoted relative to Me_4Si standard. Electronic absorption spectra were obtained with a Hewlett

Packard 8453 spectrometer. Cyclic voltammetry measurements were performed with a conventional three-electrode configuration consisting of a glassy carbon working electrode, Pt-wires auxiliary electrode and Ag/AgCl as reference electrode. All the CV measurements was performed in deoxygenated MeCN, with 0.1 M [^{n}Bu$_4$N][PF$_6$] as the supporting electrolyte. Elemental analyses were performed with a Vario EL elemental analyzer.

Theoretical calculations

All of the calculations were performed using the Gaussian 03 program package. The DFT method at the B3LYP/6-31G(d) level was used to optimize the ground-state geometries of **BTBDT1**–**BTBDT4**.

Fabrication of bulk heterojunction solar cells

The devices with the structure of ITO/PEDOT-PSS/active layer/Ca/Al, in which the active layer is a blend film of **BTBDT1**–**BTBDT4** as the electron donor and PC$_{61}$BM or PC$_{71}$BM as the electron acceptor in different weight ratio were adopted. The patterned indium tin oxide (ITO) glass was pre-cleaned in an ultrasonic bath of acetone and isopropanol, and treated in an ultraviolet-ozone chamber (Jelight Company, USA) for 30 min. A thin layer (30 nm) of poly(3,4-ethylenedioxythiophene):poly(styrene sulfonate) (PEDOT:PSS, Baytron P VP AI 4083, Germany) was spin-coated onto the ITO glass and baked at 150 ^{o}C for 30 min. A chloroform solution of a blend of **BTBDT1–BTBDT4**:PCBM was subsequently spin-coated on the PEDOT:PSS layer to form a photosensitive layer (*ca.* 80 nm). The thickness of photosensitive layer was measured using an Ambios Technology XP-2 profilometer. Calcium (*ca.* 25 nm) and aluminum (*ca.* 60 nm) layers were subsequently evaporated onto the surface of photosensitive layer under vacuum to form the negative electrode. The active area of the device was 4 mm^2. The current–voltage characteristics were measured using a computer controlled Keithley 236 Source Measure Unit. The photocurrent was measured under AM 1.5G illumination at 100 mW cm^{-2} from a xenon lamp coupled with AM 1.5G solar spectrum filters. The EQE was measured at a chopping frequency of 275 Hz with a lock-in amplifier (Stanford, SR830) during illumination with the monochromatic light from a xenon lamp.

Fabrication and characterization of organic field-effect transistors

Organic field effect transistors (OFETs) were prepared on n+Si/SiO$_2$ substrates by spin-coating process. Au source and drain electrodes were deposited on organic semiconductor films by thermal evaporation through a shadow mask with the channel length and width of 100 μm and 2 mm, respectively [27]. The thickness of the gate oxide (SiO$_2$) is 300 nm. The OFETs were characterized in the glovebox with a semiconductor parameter analyzer (Agilent 4156C). For transfer characteristics ($I_D \approx V_G$), the channel current (I_D) between the source and drain was measured as a function of gate voltage (V_G) under a constant drain voltage. For output characteristics ($I_D \sim V_{DS}$), the channel current (I_D) was measured as a function of drain voltage (V_{DS}) under a constant gate voltage (V_G) and different V_G values resulted in different curves for I_D versus V_{DS}. The field effect mobility of each transistor was calculated in the saturation regime (V_{DS} = –80 V) by plotting the square root of channel current (I_D) versus the gate voltage (V_G) and fitting the curve by equation (1), in which C_i is the capacitance of the gate oxide with a unit area .[27]

$$\mu = \frac{2L}{WC_i}\left(\frac{d\sqrt{I_D}}{dV_G}\right)^2 \quad (1)$$

Result and discussion

Synthesis and characterization

Scheme 1 depicts the synthetic routes for **BTBDT1–BTBDT4**. All of these compounds were synthesized *via* Stille coupling reaction of compounds **3**, **4**, **7** and **6** with BDT-based bis(tributylstannane) reagent, respectively. Also, compounds **3**, **4** and **7** were synthesized *via* Stille coupling reaction of 4,7-dibromobenzothiadiazole or 4,7-dibromo-5-fluorobenzothiadiazole with the corresponding tributylstannane reagent. Through Stille coupling of **4** with thiophene-derived tributylstannane and subsequent bromination reaction with NBS, **6** was obtained. All the target compounds were purified by column chromatography on silica gel and fully characterized by mass spectrometry as well as ^{1}H and ^{13}C NMR spectroscopy.

Photophysical properties

To study the potential of **BTBDT1–BTBDT4** in organic solar cells, optical properties of the newly synthesized compounds are presented. As shown in Figure 2 and Table 1, CH_2Cl_2 solutions of all compounds exhibited broad optical absorption profile with distinct high energy bands and low energy bands. The higher energy absorption bands are attributed to the localized π-π* transitions and the lower energy absorption bands can be assigned

Table 1 Absorption and CV data, energy levels and hole mobilities of BTBDT1–BTBDT4.

	λ_{max}^{abs} (nm)		E_g^a	ε^b	E_{ox}/E_{red}^c	HOMO	LUMO	μ_h
	Solution	Film	(eV)	(M^{-1} cm^{-1})	(V)	(eV)	(eV)	(cm^2 V^{-1} s^{-1})
BTBDT1	519	489,551,598	1.67	5.4×10^4	0.49/–1.17	–5.22	–3.56	3.83×10^{-6}
BTBDT2	532	550	1.72	10.4×10^4	0.52/−1.26	–5.25	–3.47	2.45×10^{-5}
BTBDT3	528	547, 585	1.69	11.5×10^4	0.50/−1.15	–5.23	–3.58	1.85×10^{-5}
BTBDT4	525	564	1.64	14.3×10^4	0.39/−1.19	–5.11	–3.54	8.37×10^{-6}

[a] Estimated from the absorption edge in the thin film. [b] Extinction coefficient at λ_{max} in solution. [c] The onset oxidation (E_{ox}) and reduction potentials (E_{red})

Cite this: DOI: 10.1039/c0xx00000x

www.rsc.org/xxxxxx

ARTICLE TYPE

to the intramolecular charge transfer (ICT). Such absorption profiles are typical of D-A architectural molecules. As shown in Fig. 2(a), **BTBDT2** and **BTBDT3** exhibited similar absorption curves in CH_2Cl_2 solutions due to their analogous molecular structures. Replacing the 3-hexylthiophene groups in **BTBDT1** by *N,N*-di-*p*-tolylbenzenamine unit resulted in a slight red shift (<10 nm) of the absorption maximum (λ_{max}) and the onset of absorption (λ_{onset}). **BTBDT4** with additional thiophene units in the middle of D-A segment of **BTBDT2** showed the highest molar absorption coefficient of 14.3×10^4 M^{-1} cm^{-1} and its absorption maximum (λ_{max}) and λ_{onset} in thin film are slightly red-shifted as compared to **BTBDT2,** together with the emergence of one more band in the high energy region. All of the compounds showed significantly red-shifted absorption spectra in thin films as compared with those in solution. More importantly, for **BTBDT1** and **BTBDT3**, the absorption spectra of their thin films exhibited a strong shoulder peak at 598 nm and 585 nm, respectively, which are due to the strong intermolecular π-π stacking in their solid state.

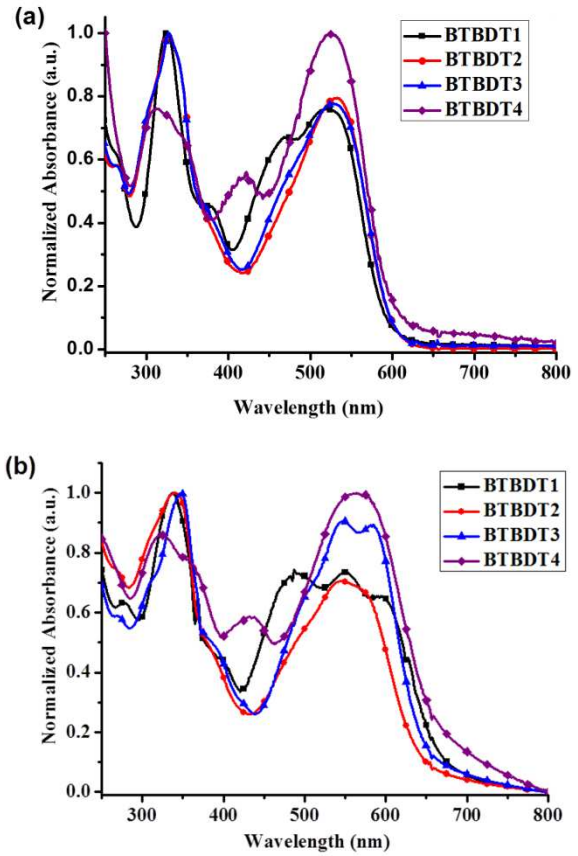

Fig. 2 Normalized absorption spectra of **BTBDT1–BTBDT4** in (a) dilute CH_2Cl_2 solution and (b) thin films on quartz substrate.

Electrochemical properties

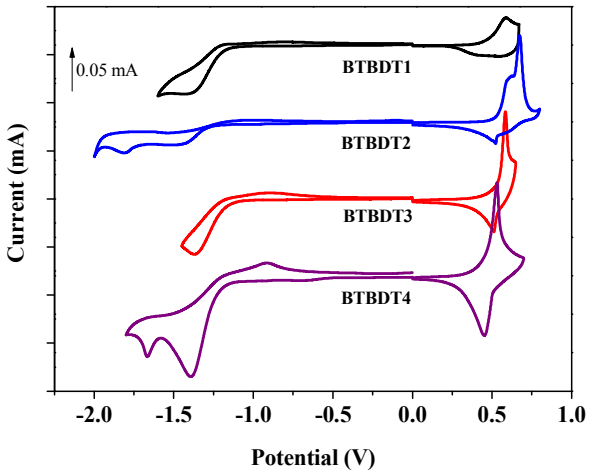

Fig. 3 Cyclic voltammograms of **BTBDT1–BTBDT4** in 0.10 M Bu_4NPF_6/CH_3CN with a scan rate 100 mV s^{-1}.

To evaluate the oxidation (E_{ox}) and reduction potentials (E_{red}) of these conjugated molecules, cyclic voltammetry (CV) was performed on their thin films on glassy carbon electrode. The highest occupied molecular orbital (HOMO) and lowest unoccupied molecular orbital (LUMO) energy levels were estimated from the onset oxidation (E_{ox}) and reduction (E_{red}) potentials by assuming the energy level of ferrocene/ferrocenium (Fc/Fc^+) to be –4.80 eV below the vacuum level. (The formal potential of Fc/Fc^+ was measured as 0.07 V against Ag/Ag^+).[28] The similar LUMO energy levels of **BTBDT1–BTBDT4** (except for **BTBDT3**) are reasonably attributed to the same BT acceptor unit for them (Fig. 3). Also, the parallel molecular backbones of **BTBDT2** and **BTBDT3** result in their similar HOMO energy levels. However, the corresponding LUMO energy level of **BTBDT3** is lower by about 0.11 eV than that of **BTBDT2**, which is reasonably attributed to the presence of the F-BT fragments in which the electron-withdrawing F group will cause **BTBDT3** reduced more easily. This is also consistent with the TDDFT data (Table S2). **BTBDT4**, which contains two more thiophene units than **BTBDT2** and **BTBDT3**, shows a little higher HOMO energy level. As the V_{oc} is proportional to the energy difference between the LUMO of the acceptor and the HOMO of the donor, the V_{oc} of **BTBDT4** is lower than those of other compounds under the same device conditions.

Theoretical studies

To understand the optical and electrochemical properties of our compounds, we have modeled the electronic structure by density functional theory (DFT) calculations using the hybrid B3LYP

exchange-correlation functional and the split-valence 6-31G(d,p) basis set.[29] Contributed by the fully planar backbone structures (considered as A-D-A or A-π-D-π-A) of all these four compounds, the electronic distributions in the frontier molecular orbitals of each molecule are spread throughout the whole π-conjugated backbone in the HOMO energy levels (Fig. 4). Moreover, the fully coplanar configuration of these backbones will facilitate the π-electron delocalization along the conjugated backbone, leading to a smaller band gap. On the contrary, in the molecular LUMO energy levels, the electron distributions of all these compounds are mostly located on the BT (or f-BT) moiety.

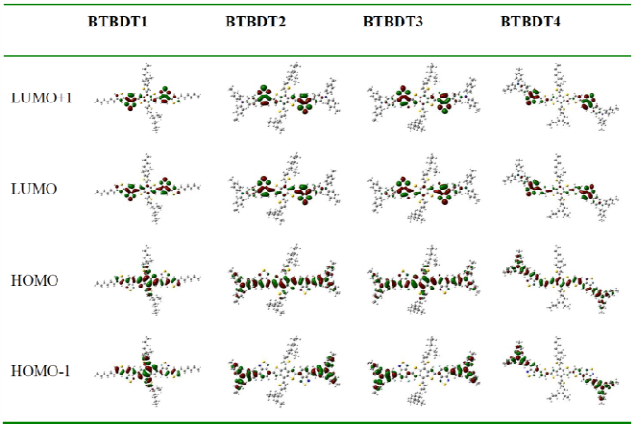

Fig. 4 DFT/B3LYP/6-31G gap orbital energy and topologies of **BTBDT1–BTBDT4**.

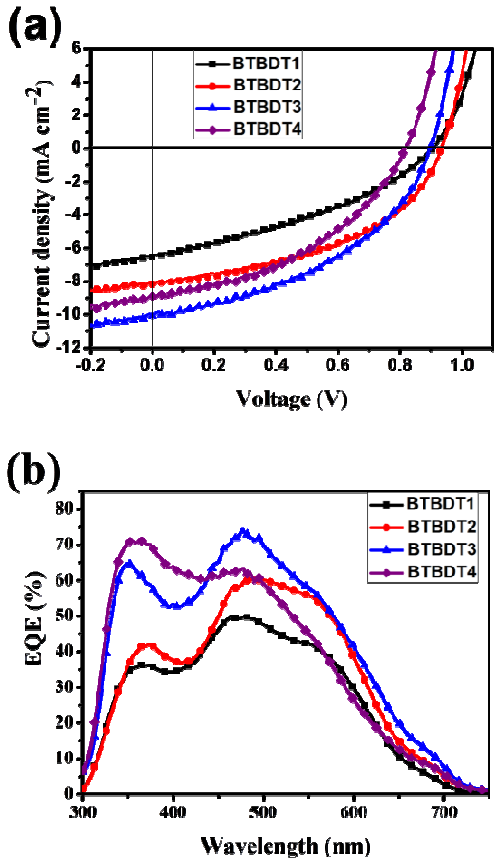

Fig. 5 (a) Current–density (*J–V*) curves and (b) EQE spectra of the devices with a ratio of **BTBDT1–BTBDT4**/$PC_{71}BM$ = 1:2 (w/w) under the illumination of AM 1.5G, 100 mW cm^{-2}.

BHJ solar cell performance

BHJ solar cells based on **BTBDT1–BTBDT4** were fabricated in a typical configuration of ITO/PEDOT-PSS/active layer/Ca/Al and their performance was tested. OSCs were optimized empirically by scrutinizing variation in the blend ratios of the compounds to $PC_{61}BM$ or $PC_{71}BM$, respectively. The resulting open-circuit voltage (V_{oc}), short-circuit current density (J_{sc}), fill factor (FF), and power conversion efficiency (PCE) values were determined from the *J-V* curves (Fig. 5), and all of the relevant solar cell performance parameters are summarized in Table 2.

Table 2 Photovoltaic properties of the OSCs based on donor/$PC_{71}BM$ (different ratio, w/w) under illumination of AM 1.5G, 100mW cm^{-2}

Donor	Donor : $PC_{71}BM$ (w/w)	V_{oc} (V)	J_{sc} (mA cm^{-2})	FF	PCE (%)
BTBDT1	1 : 1	0.92	7.12	33.2	2.18
	1 : 2	0.90	6.87	36.2	2.24
	1 : 3	0.87	6.43	35.4	1.98
BTBDT2	1 : 1	0.95	5.62	33.7	1.80
	1 : 2	0.93	8.19	46.1	3.51
	1 : 3	0.89	8.66	42.9	3.31
BTBDT3	1 : 1	0.85	8.55	34.1	2.47
	1 : 2	0.90	10.08	43.1	3.91
	1 : 3	0.89	9.68	42.2	3.64
BTBDT4	1 : 1	0.83	8.55	41.1	2.94
	1 : 2	0.82	8.89	42.6	3.10
	1 : 3	0.85	8.65	38.2	2.81

The current density versus voltage (*J-V*) curves of **BTBDT1–BTBDT4**/$PC_{71}BM$ with different weight blend ratios are illustrated in Fig. 5(a) and the related EQE curves are shown in Fig. 5(b), respectively. As the donor/$PC_{71}BM$ blend ratio was increased from 1:1 to 1:2, the optimized device gave the best PCE for each compound. Among them, **BTBDT3** showed the highest PCE of 3.91%, accompanied by a V_{oc} of 0.90 V, a J_{sc} of 10.08 mA cm^{-2}, and FF of 43.1%. With a further increase in the content of $PC_{71}BM$, the corresponding J_{sc} and FF values together with the PCE value in each compound were decreased (except for the J_{sc} in **BTBDT2**).

For efficient photovoltaic devices, the charge-carrier mobility, as an essential property for OSCs, is one of the important factors that affect the J_{sc} in the devices. In order to enhance charge carrier transport in the active layer as well as to reduce the recombination of photocurrent in solar cells, a high hole mobility is required for the electron donor. The hole mobilities of these BDT-based compounds were studied using organic field-effect transistors (OFETs). The mobilities calculated at V_{DS} = – 80 V of **BTBDT1–BTBDT4** are given in Table 1 and typical p-type characteristics were observed for all compounds (Fig. S2). The field-effect hole mobilities of 3.83×10^{-6} cm^2 V^{-1} s^{-1}, 2.45×10^{-5} cm^2 V^{-1} s^{-1}, 1.85×10^{-5} cm^2 V^{-1} s^{-1} and 8.37×10^{-6} cm^2 V^{-1} s^{-1} were observed in OFETs based on **BTBDT1–BTBDT4**, respectively. In general, addition of the strongly electron-donating arylamino group tends to increase the hole mobility in the series. Also, the hole mobilities of **BTBDT2** and **BTBDT3** are comparatively higher than the others, and this is consistent

with the relatively higher J_{sc} of 8.19 mA cm^{-2} and 10.08 mA cm^{-2} in their photovoltaic devices, as compared with those from **BTBDT1** and **BTBDT4**. In addition, the FF value of the OSCs based on **BTBDT2** and **BTBDT3** (at 1:2 ratio, w/w) were notably higher than the other two, which could be attributed to their higher hole mobilities.[30] While extension of the conjugation length of **BTBDT4** is expected to lead to a red-shifted and stronger absorption which is favorable for improving the solar cells, the lower V_{oc} of **BTBDT4** due to its higher HOMO level is actually the main reason for its lower PCE than those of **BTBDT2** and **BTBDT3**.

Since the photoconversion efficiencies are also greatly influenced by the morphologies of active layer in thin films, we also investigated the morphology of the **BTBDT1**–**BTBDT4**/$PC_{71}BM$ (1:2, w/w) blend films by atomic force microscopy (AFM) techniques (see Fig. S3, Supporting Information). The surfaces of these four blend films are quite smooth with similar root-mean-square (rms) values of 0.366, 0.283, 0.307 and 0.296 nm for **BTBDT1**/$PC_{71}BM$, **BTBDT2**/$PC_{71}BM$, **BTBDT3**/$PC_{71}BM$ and **BTBDT4**/$PC_{71}BM$, respectively. Thus, the film morphology is not the key factor in governing the overall PCE of the OSCs.

The EQE value refers to the percentage of incident photons in a given wavelength divided by the charges that are finally carried to an external circuit. All the EQE curves based on **BTBDT1**–**BTBDT4**/$PC_{71}BM$ were broad in response covering 300–700 nm, consistent with the corresponding optical absorption bands. Among them, the peak EQE of 73% at 480 nm was achieved by using **BTBDT3**/$PC_{71}BM$ blend at 1:2 blend ratio. The calculated photocurrent densities from EQE spectra are consistent with those obtained from *J–V* measurements.

Conclusions

A series of new organic small molecules based on the BDT-T unit as the central donor group and BT unit or F-BT as the acceptor were synthesized and characterized and, their structure-property relationships have been investigated. Among them, **BTBDT1** was constructed by 3-hexylthiophene unit as the end-capping group. **BTBDT2–BTBDT4** contain *N,N*-di-*p*-tolylbenzenamine unit as the end-capping group which can enhance the hole mobility of the blend film. The similar LUMO energy levels of **BTBDT1, BTBDT2** and **BTBDT4** are reasonably attributed to the similar BT acceptor unit in them. For **BTBDT3**, the fluoro-containing BT (F-BT) unit relative to BT unit will influence its LUMO energy level. As shown in the representative orbital energy diagrams done by the DFT calculations, these molecules possess fully planar backbone structures (considered as A-D-A or A-π-D-π-A). More importantly, the electronic distributions in their HOMO energy levels of each molecule are spread throughout the whole π-conjugated backbone. For BHJ solar cells fabricated by **BTBDT1–BTBDT4**, dye **BTBDT3** shows the best performance with a high PCE of 3.91%. This work demonstrates that alkylthiophene-substituted organic small molecules derived from BDT are promising donor materials for solution-processed organic solar cells.

Acknowledgements

We thank Hong Kong Baptist University (FRG2/12-13/083), Hong Kong Research Grants Council (HKBU202410), The Science, Technology and Innovation Committee of Shenzhen Municipality (JCYJ20120829154440583) for financial support. The work described in this paper was also partially supported by a grant from the Research Grants Council of the Hong Kong Special Administrative Region, China (Project No. T23-713/11). H. Li thanks the 111 Project and Beijing Engineering Research Center of Food Environment and Public Health from Minzu University of China (No. B08044 and No.10301-01404026) for financial support. We gratefully acknowledge the financial support from the National Science Council of Taiwan (NSC 102-2113-M-845-001) and the project of the specific research fields in the University of Taipei, Taiwan. The work was also supported by Partner State Key Laboratory of Environmental and Biological Analysis (SKLP-14-15-P011) and Strategic Development Fund of HKBU.

Notes and references

[1] G. Yu, J. Gao, J. C. Hummelen, F. Wudl and A. J. Heeger, *Science*, 1995, **270**, 1789.
[2] Y. J. Cheng, S. H. Yang and C. S. Hsu, *Chem. Rev*., 2009, **109**, 5868.
[3] G. Dennler, M. C. Scharber and C. J. Brabec, *Adv. Mater*., 2009, **21**, 1323.
[4] J. W. Chen and Y. Cao, *Acc. Chem. Res*., 2009, **42**, 1709.
[5] R. Fitzner, E. Mena-Osteritz, A. Mishra, G. Schulz, E. Reinold, M. Weil, C. Koerner, H. Ziehlke, C. Elschner, K. Leo, M. Riede, M. Pfeiffer, C. Uhrich and P. Baeuerle, *J. Am. Chem. Soc*., 2012, **134**, 11064.
[6] H. X. Zhou, L. Q. Yang and W. You, *Macromolecules*, 2012, **45**, 607.
[7] Y. F. Li, *Acc. Chem. Res*., 2012, **45**, 723.
[8] A. Facchetti, *Chem. Mater*., 2011, 23, 733.
[9] P. M. Beaujuge and J. M. J. Frechet, *J. Am. Chem. Soc*., 2011, **133**, 20009.
[10] (a) Z. C. He, C. M. Zhong, S. J. Su, M. Xu, H. B. Wu and Y. Cao, *Nat. Photonics*, 2012, **6**, 591; (b) W.-Y. Wong and C.-L. Ho, *Acc. Chem. Res*., 2010, 43, 1246; (c) Z. C. He, C. M. Zhong, X. Huang, W.-Y. Wong, H. B. Wu, L. W. Chen, S. J. Su and Y. Cao, *Adv. Mater*., 2011, **23**, 4636.
[11] B. Walker, C. Kim and T.-Q. Nguyen, *Chem. Mater*., 2011, **23**, 470.
[12] Y. Lin, Y. Li and X. Zhan, *Chem. Soc. Rev*., 2012, **41**, 4245.
[13] A. Mishra and P. Baeuerle, *Angew. Chem., Int. Ed*., 2012, **51**, 2020.
[14] (a) Y. S. Liu, X. J. Wan, B. Yin, J. Y. Zhou, G. K. Long, J. G. Tian, J. B. You, Y. Yang and Y. S. Chen, *Adv. Energ. Mater.*, 2011, **1**, 771; (b) J. Y. Zhou, X. J. Wan, Y. S. Liu, Y. Zuo, Z. Li, G. R. He, G. K. Long, W. Ni, C. X. Li, X. C. Su and Y. S. Chen. *J. Am. Chem. Soc*., 2012, **134**, 16345; (c) C. H. Cui, J. Min, C.-L. Ho, T. Ameri, P. Yang, J. Z. Zhao, C. J. Brabec and W.-Y. Wong, *Chem. Commun*., 2013, 49, 4409.
[15] (a) O. P. Lee, A. T. Yiu, P. M. Beaujuge, C. H. Woo, T. W. Holcombe, J. E. Millstone, J. D. Douglas, M. S. Chen and J. M. J. Frechet, *Adv. Mater*., 2011, **23**, 5359; (b) B. Walker, A. B. Tomayo, X. D. Dang, P. Zalar, J. H. Seo, A. Garcia, M. Tantiwiwat and T.- Q. Nguyen, *Adv. Funct. Mater*., 2009, **19**, 3063; (c) S. Loser, C. J. Bruns, H. Miyauchi, R. P. Ortiz, A. Facchetti, S. I. Stupp and T. J. Marks, *J. Am. Chem. Soc*., 2011, **133**, 8142; (d) D. Sahu, C.-H. Tsai, H-Y. Wei, K.-C. Ho, F.-C. Chang and C.-W. Chu, *J. Mater. Chem*., 2012, **22**, 7945.
[16] H. X. Shang, H. J. Fan, Y. Liu, W. P. Hu, Y. F. Li and X. W. Zhan, *Adv. Mater*., 2011, **23**, 1554; (b) Y. Z. Lin, Z. G. Zhang, H. T. Bai, Y. F. Li and X. W. Zhan, *Chem. Commun*., 2012, **48**, 9655; (c) Y. Z. Lin, Z. G. Zhang, Y. F. Li, D. B. Zhu and X. W. Zhan, *J. Mater. Chem. A*, 2013, **1**, 5128.

[17] (a) J. Peet, J. Y. Kim, N. E. Coates, W. L. Ma, D. Moses, A. J. Heeger and G. C. Bazan, *Nat. Mater*., 2007, **6**, 497; (b) R. C. Coffin, J. Peet, J. Rogers and G. C. Bazan, *Nat. Chem*., 2009, **1**, 657; (c) D. Muhlbacher, M. Scharber, M. Morana, Z. Zhu, D. Waller, R. Gaudiana and C. Brabec, *Adv. Mater*., 2006, **18**, 2884.

[18] Q. Q. Shi, P. Cheng, Y. F. Li and X. W. Zhan, *Adv. Energy Mater*., 2012, **2**, 63.

[19] (a) J. H. Hou, H.-Y. Chen, S. Q. Zhang, G. Li and Y. Yang, *J. Am. Chem. Soc*., 2008, **130**, 16144; (b) Y. M. Sun, G. C. Welch, W. L. Leong, C. J. Takacs, G. C. Bazan and A. J. Heeger, *Nat. Mater*., 2012, **11**, 44; (c) J. Y. Zhou, X. J. Wan, Y. S. Liu, G. K. Long, F. Wang, Z. Li, Y. Zuo, C. X. Li and Y. S. Chen, *Chem. Mater*., 2011, 23, 4666.

[20] T. Bura, N. Leclerc, S. Fall, P. Leveque, T. Heiser, P. Retailleau, S. Rihn, A. Mirloup and R. Ziessel, *J. Am. Chem. Soc.*, 2012, **134**, 17404.

[21] A. K. K. Kyaw, D. H. Wang, V. Gupta, W. L. Leong, L. Ke, G. C. Bazan and A. J. Heeger, *ACS Nano*, 2013, **7**, 4569.

[22] (a) L. Huo, S. Zhang, X. Guo, F. Xu, Y. Li and J. Hou, *Angew. Chem., Int. Ed*., 2011, **50**, 9697; (b) H.-Y. Chen, J. Hou, S. Zhang, Y. Liang, G. Yang, Y. Yang, L. Yu, Y. Wu and G. Li, *Nat. Photonics*, 2009, **3**, 649; (c) H. Zhou, L. Yang, A. C. Stuart, S. C. Price, S. Liu and W. You, *Angew. Chem., Int. Ed*., 2011, **50**, 2995; (d) S. C. Price, A. C. Stuart, L. Yang, H. Zhou and W. You, *J. Am. Chem. Soc*., 2011, **133**, 4625; (e) T.-Y. Chu, J. Lu, S. Beaupre, Y. Zhang, J.-R. Pouliot, S. Wakim, J. Zhou, M. Leclerc, Z. Li, J. Ding and Y. Tao, *J. Am. Chem. Soc*., 2011, **133**, 4250; (f) L. Dou, J. You, J. Yang, C.-C. Chen, Y. He, S. Murase, T. Moriarty, K. Emery, G. Li and Y. Yang, *Nat. Photonics*, 2012, **6**, 180.

[23] (a) Y. S. Liu, X. J. Wan, F. Wang, J. Y. Zhou, G. K. Long, J. G. Tian and Y. S. Chen, *Adv. Mater*., 2011, **23**, 5387; (b) P. Dutta, J. Kim, S. H. Eom, W.-H. Lee, I. N. Kang and S.-H. Lee, *ACS Appl. Mater. Interfaces*, 2012, **4**, 6669.

[24] (a) H. C. Chen, Y. H. Chen, C. C. Liu, Y. C. Chien, S. W. Chou and P. T. Chou, *Chem. Mater*., 2012, **24**, 4766; (b) L. J. Huo and J. H. Hou, *Polym. Chem*., 2011, **2**, 2453; (c) J. Huang, C. Zhan, X. Zhang, Y. Zhao, Z. Lu, H. Jia, B. Jiang, J. Ye, S. Zhang, A. Tang, Y. Liu, Q. Pei and J. Yao, *ACS Appl. Mater. Interfaces*, 2013, **5**, 2033; (d) S. Shen, P. Jiang, C. He, J. Zhang, P. Shen, Y. Zhang, Y. Yi, Z. Zhang, Z. Li and Y. Li, *Chem. Mater.*, 2013, **25**, 2274; (e) Y. Lin, L. Ma, Y. Li, Y.Liu, D. Zhu and X. Zhan, *Adv. Energy Mater.*, 2013, **3**, 1166; (f) J. Zhou, Y. Zuo, X. Wan, G. Long, Q. Zhang, W. Ni, Y. Liu, Z. Li, G. He, C. Li, B. Kan, M. Li and Y. Chen, *J. Am. Chem. Soc.*, 2013, **135**, 8484; (g) J. Zhou, X. Wan, Y. Liu, Y. Zuo, Z. Li, G. He, G. Long, W. Ni, C. Li, X. Su and Y. Chen, *J. Am. Chem. Soc.*, 2012, **134**, 16345; (h) Y. Liu, C.-C. Chen, Z. Hong, J. Gao, Y. Yang, H. Zhou, L. Dou, G. Li and Y. Yang, *Sci. Rep.*, 2013, **3**, 3356; (i) Z. Du, Y. Chen, W. Chen, S. Qiao, S. Wen, Q. Liu, D. Zhu, M. Sun and R. Yang, *Chem. Asian J.*, 2014, DOI: 10.1002/asia.201402467.

[25] (a) S. Wong, H. Ma, A. K. Y. Jen, R. Barto and C. W. Frank, *Macromolecules*, 2003, **36**, 8001; (b) K. Reichenbacher, H. I. Suss and J. Hulliger, *Chem. Soc. Rev*., 2005, **34**, 22.

[26] F. R. Dai, H. M. Zhan, Q. Liu, Y. Y. Fu, J. H. Liu, Q. W. Wang, Z. Y. Xie, L. X. Wang, F. Yan and W.-Y. Wong, *Chem. Eur. J*., 2012, **18**, 1502.

[27] Z. H. Sun, J. H. Li, C. M. Liu, S. H. Yang and F. Yan, *Adv. Mater.*, 2011, **23**, 3648.

[28] B. C. Thompson, Y. G. Kim and J. R. Reynolds, *Macromolecules*, 2005, **38**, 5359.

[29] M. J. Frisch, G. W. Trucks, H. B. Schlegel, G. E. Scuseria, M. A. Robb, J. R. Cheeseman, J. A. Montgomery, Jr, T. Vreven, K. N. Kudin, J. C. Burant, J. M. Millam, S. S. Iyengar, J. Tomasi, V. Barone, B. Mennucci, M. Cossi, G. Scalmani, N. Rega, G. A. Petersson, H. Nakatsuji, M. Hada, M. Ehara, K. Toyota, R. Fukuda, J. Hasegawa, M. Ishida, T. Nakajima, Y. Honda, O. Kitao, H. Nakai, M. Klene, X. Li, J. E. Knox, H. P. Hratchian, J. B. Cross, C. Adamo, J. Jaramillo, R. Gomperts, R. E. Stratmann, O. Yazyev, A. J. Austin, R. Cammi, C. Pomelli, J. W. Ochterski, P. Y. Ayala, K. Morokuma, G. A. Voth, P. Salvador, J. J. Dannenberg, V. G. Zakrzewski, S. Dapprich, A. D. Daniels, M. C. Strain, O. Farkas, D. K. Malick, A. D. Rabuck, K. Raghavachari, J. B. Foresman, J. V. Ortiz, Q. Cui, A. G. Baboul, S. Clifford, J. Cioslowski, B. B. Stefanov, G. Liu, A. Liashenko, P. Piskorz, I. Komaromi, R. L. Martin, D. J. Fox, T. Keith, M. A. Al-Laham, C. Y. Peng, A. Nanayakkara, M. Challacombe, P. M. W. Gill, B. Johnson, W. Chen, M. W. Wong, C. Gonzalez, and J. A. Pople, Gaussian 03, Revision B.03, Gaussian, Inc., Pittsburgh PA, 2003.

[30] C. Cui, W.-Y. Wong and Y. Li, *Energy Environ. Sci.*, 2014, **7**, 2276.

[a] *State Key Laboratory of Polymer Physics and Chemistry, Changchun Institute of Applied Chemistry, Chinese Academy of Sciences, Changchun 130022, PR China*

[b] *Institute of Molecular Functional Materials, Partner State Key Laboratory of Environmental and Biological Analysis, Department of Chemistry and Institute of Advanced Materials, Hong Kong Baptist University, Waterloo Road, Kowloon Tong, Hong Kong, PR China*
E-mail: rwywong@hkbu.edu.hk; Tel.: +852 34117074; fax: 852 34117348.

[c] *State Key Laboratory of Alternate Electrical Power System with Renewable Energy Sources, Beijing Key Laboratory of Energy Security and Clean Utilization, North China Electric Power University, Beijing 102206, PR China*
Email: tanzhanao@ncepu.edu.cn; Tel./fax: +86 10 61772186.

[d] *Department of Applied Physics, The Hong Kong Polytechnic University, Hung Hom, Hong Kong, PR China*

[e] *Institute of Theoretical Chemistry, State Key Laboratory of Theoretical and Computational Chemistry, Jilin University, Changchun 130023, PR China*

[f] *College of Life and Environmental Sciences & Beijing Engineering Research Center of Food Environment and Public Health, Minzu University of China, Beijing, 100081, PR China*

[g] *Department of Applied Physics and Chemistry, University of Taipei, Taipei 100, Taiwan.*
E-mail: yhlo@utaipei.edu.tw; Tel.: +886 2 23113040; fax: +886 2 23897641.

[h] *Clinical Division, School of Chinese Medicine, Hong Kong Baptist University, Waterloo Road, Hong Kong, P.R. China.*

† Electronic Supplementary Information (ESI) available. See DOI: 10.1039/b000000x/